Ideal Surface Geometries of Nucleating Agents to Enhance Cell Nucleation in Polymeric Foaming Processes

Siu N. Leung,[1] Anson Wong,[1] Chul B. Park,[1] Jin Ho Zong[2]

[1]*Department of Mechanical & Industrial Engineering, University of Toronto, Toronto, Ontario, Canada*
[2]*Department of Materials, Mechanical & Automation Engineering, Yanbian University of Science & Technology, Yanji, Jilin, People's Republic of China*

Received 1 October 2007; accepted 2 January 2008
DOI 10.1002/app.28038
Published online 17 March 2008 in Wiley InterScience (www.interscience.wiley.com).

ABSTRACT: Ideal nucleating agents are expected to improve the cell morphology of plastics foams (i.e., increasing the cell density, reducing the cell size, and narrowing cell-size distribution) by providing heterogeneous nucleation sites. A nucleating agent's surface geometry is one factor that governs its nucleating power. This paper discusses the surface geometry of an ideal nucleating agent. On the basis of computer simulations of a batch foaming process using polystyrene and carbon dioxide, we found that nucleating agents having numerous crevices with small semiconical angles are the most desirable for polymeric foaming processes. © 2008 Wiley Periodicals, Inc. J Appl Polym Sci 108: 3997–4003, 2008

Key words: polymeric foam; heterogeneous nucleation; nucleating agent; surface geometry; foaming simulation

INTRODUCTION

Plastic foams with high cell densities, small cell sizes, and narrow cell-size distributions are widely used because they offer improved mechanical,[1–6] thermal,[7] acoustical,[7] and optical[8] properties. Moreover, polymeric foaming process allow manufacturers to reduce their raw material costs, which have risen dramatically in recent years due to ongoing increases in the price of plastic resins. Nucleating agents are commonly used for controlling cell nucleation in the production of high-quality foam products. The effects of nucleating agents on cell nucleation were studied by Hansen et al.[9–10] in the 1960s. Later studies identified effective nucleating agents for plastic foaming processes, such as azodicarbonamide,[11] calcium carbonate,[11–12] calcium stearate,[11,13–14] magnesium silicate,[15] the mixture of citric acid and sodium bicarbonate,[11,16–19] rubber particles,[20–22] sodium benzoate,[23] stearic acid,[24] silica products,[12,25] talc[11,13,16–17,26–28], and zinc stearate.[11,24] Recent studies also demonstrated the use of nanoparticles (e.g., nanoclay,[29–32] carbon nanofibers,[33] and single-walled carbon nanotubes[33]) as nucleating agents.

In polymeric foaming processes, the choice of nucleating agent to be added to the polymer matrix is often governed by experience and trial-and-error. As a qualitative guideline, McClurg proposed a set of criteria for ideal nucleating agents[34] which include:

i. Nucleation on ideal nucleating agents should be energetically favorable relative to homogeneous nucleation in the bulk of the polymer/gas solution and any other unintentional heterogeneous nucleation on other additives and contaminants in the polymer matrix or on the surface of the internal walls of the equipment.
ii. Ideal nucleating agents should have uniform sizes, surface geometries, and surface properties.
iii. Ideal nucleating agents should be easily dispersible.

Leung et al.[35] also demonstrated that the surface geometry of a heterogeneous nucleating site is a critical factor governing the free energy barrier to nucleating a bubble heterogeneously. Therefore, it is meaningful to investigate, in detail, the effects of surface geometries on heterogeneous nucleation, and thereby on the foam structures.

In this work, based on the proposed modified nucleation theory and the simulation approach adopted in our previous study,[35,36] a series of computer simulations of bubble nucleation and the subsequent bubble growth processes were conducted to study the effects on the foaming process of the surface geometry of nucleating agents and the uniformity of the geometry.

Theoretical framework

Modified nucleation theory

According to the classical nucleation theory, the heterogeneous nucleation rate, J_{het}, depends on the

Correspondence to: C. B. Park (park@mie.utoronto.ca).

Journal of Applied Polymer Science, Vol. 108, 3997–4003 (2008)

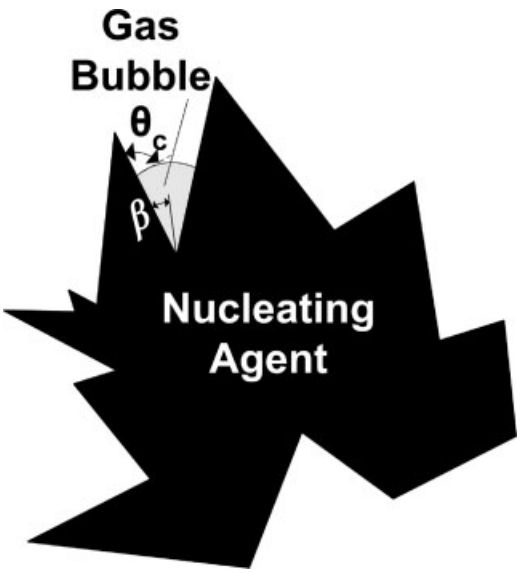

Figure 1 Surface geometry of nucleating agents with rugged surface.

surface geometry of the nucleating site.[35–37] In general, the heterogeneous nucleation rate, J_{het}, is given by[35,38]

$$J_{het} = N^{\frac{2}{3}} Q \sqrt{\frac{2\gamma_{lg}}{\pi m F}} \exp\left(-\frac{16\pi {\gamma_{lg}}^3 F}{3k_B T_{sys}\left(P_{bub,cr} - P_{sys}\right)^2} \right) \quad (1)$$

where N is the number of gas molecules per unit volume; γ_{lg} is the surface tension at the liquid-gas interface; m is the molecular mass of the dissolved gas molecules; k_B is the Boltzmann constant; T_{sys} is the processing temperature; $P_{bub,cr}$ is the bubble pressure of a critical bubble; P_{sys} is the system pressure; F is the ratio of the volume of the heterogeneously nucleated bubble on the nucleating site to the volume of a spherical bubble with the same radius; and Q is the ratio of the surface area of the liquid-gas interface of the heterogeneously nucleated bubble to the surface area of a spherical bubble with the same radius. Both F and Q depend on the surface geometry of the nucleating agents.

At the microscopic level, some nucleating agents (e.g., talc) or other unintentional heterogeneous nucleating sites (e.g., the walls of the processing equipment) have irregular surface geometries. For mathematical simplicity, it is assumed that the surface geometry can be approximated by a series of conical cavities, as shown in Figure 1, with different semiconical angles β. For bubbles nucleated in conical cavities, F and Q are functions of the contact angle θ_c and β. θ_c is the angle between the bubble surface and the solid surface being measured in the liquid phase. These geometric factors are given by[35–37]

$$F(\theta_c,\beta) = \frac{1}{4}\left\{ 2 - 2\sin(\theta_c - \beta) + \frac{\cos\theta_c \cos^2(\theta_c - \beta)}{\sin\beta} \right\} \quad (2)$$

$$Q(\theta_c,\beta) = \frac{1 - \sin(\theta_c - \beta)}{2} \quad (3)$$

Based on the idea proposed by Leung et al.[35] that the sizes of β follow a probability density function, ρ_β, the heterogeneous nucleation rate is given by

$$J_{het} = \int_\beta \rho_\beta(\beta) N^{\frac{2}{3}} Q(\theta_c,\beta) \sqrt{\frac{2\gamma_{lg}}{\pi m F(\theta_c,\beta)}} \exp\left(-\frac{16\pi {\gamma_{lg}}^3 F(\theta_c,\beta)}{3k_B T_{sys}\left(P_{bub,cr} - P_{sys}\right)^2} \right) d\beta \quad (4)$$

Bubble growth model

The bubble growth simulation was conducted using the model and approach presented by Leung et al.[39] The computer simulation considered each bubble to be surrounded by a finite shell of viscoelastic fluid containing a limited amount of gas (Fig. 2). The simulation further assumed the nucleated bubbles to be evenly distributed in the foam. The complete set of governing equations for the bubble growth process (i.e., mass balance equation, momentum equation, constitutive equations, and diffusion equation) and

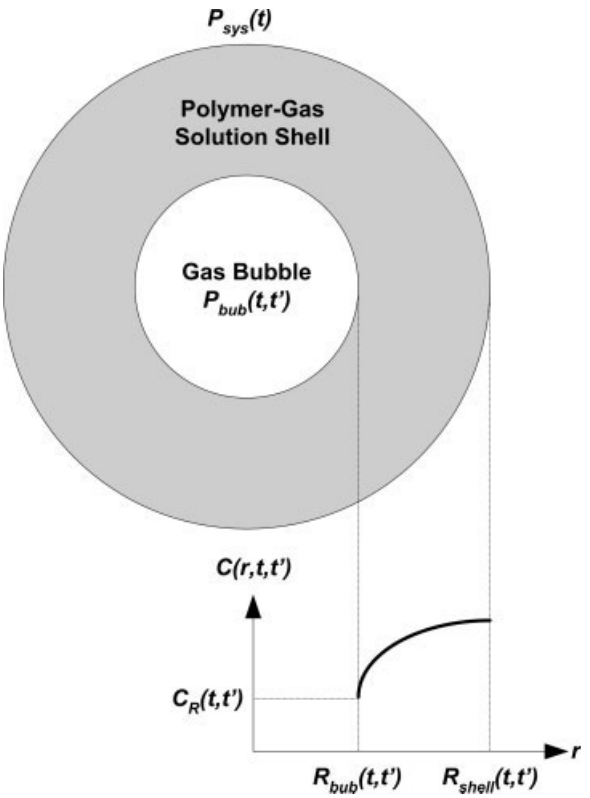

Figure 2 Cell model in bubble growth simulation system.

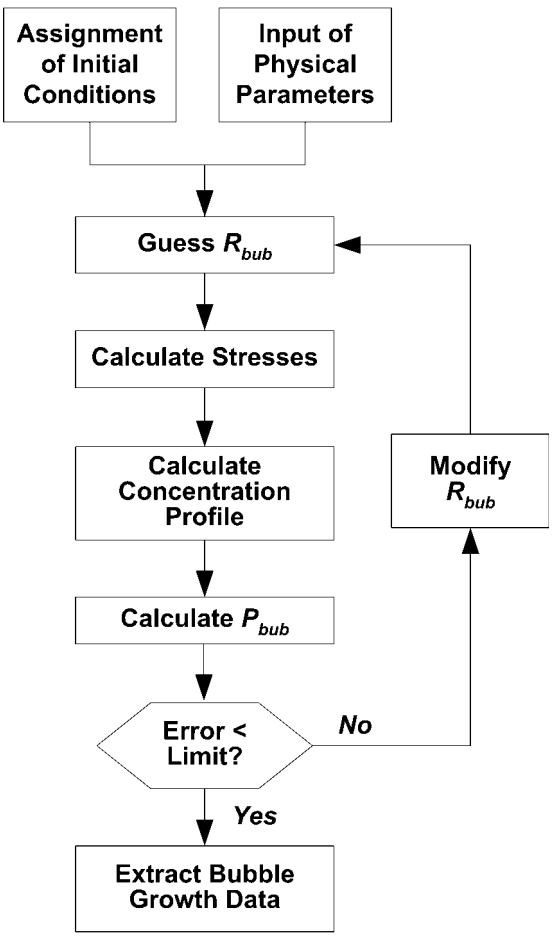

Figure 3 Bubble growth simulation algorithm.

the simulation algorithm, which is illustrated in Figure 3, are described in detail by Leung et al.[39]

Overall foaming simulation model

The effects of surface geometries on foaming behaviors can be analyzed using the nucleation theories and bubble growth model described above. Since the nucleation rate is not constant during the foaming process, the cell-population density with respect to the unfoamed polymer volume, N_{unfoam}, was determined by integrating the total nucleation rate over time using eq. (5):

$$N_{unfoam}(t) = \int_0^t [J_{hom}(t') + A_{het}J_{het}(t')]dt \quad (5)$$

Here A_{het} is the surface area of the nucleating agents per unit volume of polymer-gas solution, and J_{hom} is the homogeneous nucleation rate:

$$J_{hom} = N\sqrt{\frac{2\gamma_{lg}}{\pi m}}\exp\left(-\frac{16\pi{\gamma_{lg}}^3}{3k_BT_{sys}\left(P_{bub,cr}-P_{sys}\right)^2}\right) \quad (6)$$

Furthermore, by assuming that the ideal gas law can be applied to the gas inside a nucleated bubble, the average dissolved gas concentration remaining in the polymer-gas solution, $C_{avg}(t)$, was determined by

$$C_{avg}(t) = C_0 - \int_0^t \frac{4\pi R_{bub}(t,t')^3 P_{bub}(t,t')}{3R_gT}[J(t')]dt' \quad (7)$$

The calculated $C_{avg}(t)$ for each time step was used to modify the values of N, γ_{lg}, and $P_{bub,cr}$ in eqs. (4) and (6) when determining the total nucleation rate. The overall foaming simulation algorithm is illustrated in Figure 4.

Methodology

This study of the effects of the surface geometry of nucleating agents on heterogeneous nucleation used the overall foaming model discussed in the previous section to simulate PS/CO_2 polymeric foaming systems. The foaming systems were assumed to have

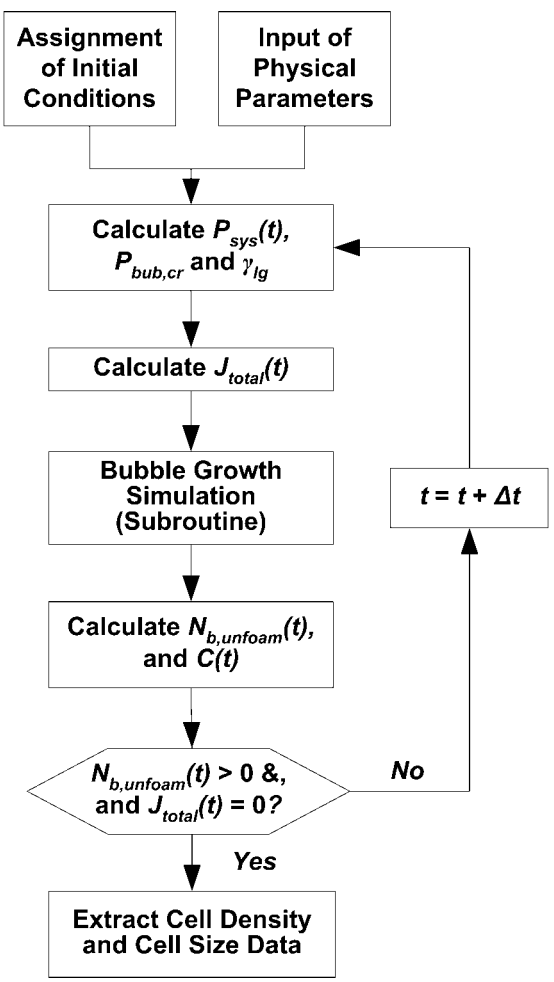

Figure 4 Overall foaming simulation algorithm.

conical nucleation sites with the sizes of β stochastically determined using various ρ_β. A simulation was run for each ρ_β, and the cell density and cell size distribution for each case was then extracted. To isolate the effects of different surface geometries in nucleating agents on nucleation behaviors, several experimental parameters were kept constant throughout all simulations: the pressure drop rate was −50 MPa/s, the CO_2 gas content was 5 wt %, and the processing temperature was 140°C. The values of $P_{bub,cr}$ were calculated using the Sanchez-Lacombe Equation of State[40] and the thermodynamic equilibrium condition from Leung et al.[36] Furthermore, θ_c was kept constant at 85.7° and A_{het} was kept constant at 10,000 m^2/m^3 throughout all simulations.[41] This value of A_{het} was obtained via an order-of-magnitude argument: (1) It was assumed that nucleating agents accounted for 5% of the total weight of the PS/CO_2 solution. (2) Using the specific gravity of talc at 2.8 as a reference, the percentage of nucleating agents by volume in the PS/CO_2 solution was calculated. (3) By approximating all nucleating agents as spheres of 1.7 μm in radius, an estimate of A_{het} was determined. As mentioned earlier, this study aimed to investigate the effects of surface geometries by varying β only. Since β is independent of A_{het}, any imprecision in the value of A_{het} should not undermine the validity of the analyses, as long as this value was kept constant throughout all simulations. This argument justifies the use of a rough estimate for A_{het}. On the other hand, θ_c cannot be estimated since θ_c depends strongly on the nucleating surface. Because such data is unavailable, the value for θ_c was obtained by the least square fit so that the experimentally observed cell density and the computer-simulated cell density can be matched for PS/CO_2 foaming under the same processing conditions.[41] From eqs. (2) and (4), it is evident that F and hence J_{het} depend on θ_c. Therefore, it should be emphasized that this study is only valid in the vicinity of the chosen θ_c. Further investigation is needed to study the effects of different θ_c.

It was assumed that β would follow one of two types of ρ_β: a uniform distribution or a series of modified normal distributions. The uniform ρ_β used was based on the assumption that R_{het} could take any value from 0° to 90° [i.e., ρ_β = U(0°,90°)]. Each of the modified normal distributions used was obtained by imposing lower and upper limits at 0° and 90°, respectively, to a probability density function of a normal distribution [i.e., N(μ,σ)] having a specified mean μ and standard deviation σ. This modified normal ρ_β, denoted as N*(μ,σ) in this study, was adopted to study the effects of skewness (i.e., μ) and dispersion (i.e., σ) in ρ_β on foaming behaviors. In order that the total area under each ρ_β equal 1, each ρ_β = N*(μ,σ) was divided by the total area under the corresponding N(μ,σ) distribution between the lower and upper limit of 0° and 90°. Note that the mean and standard deviation of each N*(μ,σ) (listed in Table I) are not the same as those of the corresponding N(μ,σ) due to the enforcement of the upper and lower limits. However, μ and σ dictate the skewness and dispersion of each ρ_β. In this study, three groups of N*(μ,σ) distributions were considered (refer to Figs. 5a-c):

TABLE I
Real Mean and Standard Derivation of the ρ_β Distribution

Case	Mean	Standard derivation
N*(15°,5°)	15.0°	5.0°
N*(30°,5°)	30.0°	5.0°
N*(45°,5°)	45.0°	5.0°
N*(15°,15°)	19.3°	11.9°
N*(30°,15°)	30.8°	14.1°
N*(45°,15°)	45.0°	14.8°
N*(15°,45°)	36.5°	23.5°
N*(30°,45°)	40.7°	24.1°
N*(45°,45°)	45.0°	24.3°
U(0°,90°)	45.0°	26.0°

i. N^*(15°,5°), N^*(30°,5°), N^*(45°,5°), U(0°,90°)
ii. N^*(15°,15°), N^*(30°,15°), N^*(45°,15°), U(0°,90°)
iii. N^*(15°,45°), N^*(30°,45°), N^*(45°,45°), U(0°,90°)

Note that U(0°,90°) was added in each case to study the convergence of the modified normal distribution and the uniform distribution at large σ. Using these ρ_β, the expected value of heterogeneous nucleation rate at each foaming simulation time step was then calculated using eq. (4). Afterward, N_{unfoam} was determined using eq. (5) to obtain the cell density and cell size distribution data for each case.

RESULTS AND DISCUSSION

Effect of β distribution on cell density

As mentioned earlier, plastic foams with a high cell density, N_{unfoam}, are desirable. From Figure 6, it is evident that N_{unfoam} depends strongly on the distribution of the semiconical angle β. That is, nucleating agents with conical crevices with small β can lead to foams with higher cell density, because F takes on smaller values at small β [see eq. (2)]. A decrease in F lowers the activation energies for cell nucleation, leading to an increase in the cell nucleation rate and ultimately an increase in cell density. This effect of β on cell density is significant when σ is small (i.e., σ = 5°); in this case, cell density increased by two orders of magnitude when μ was shifted from 45° to

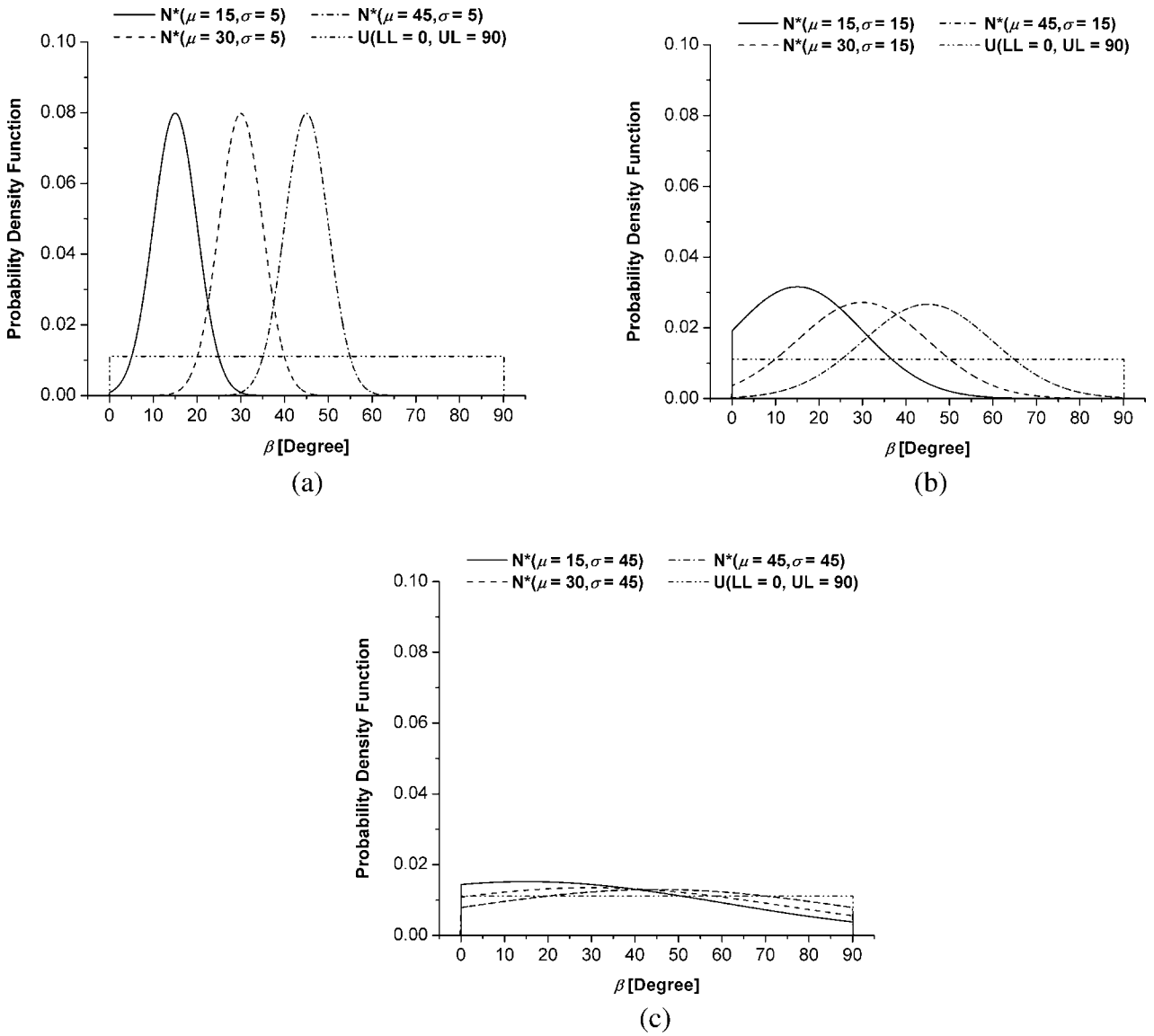

Figure 5 (a) Probability density functions of N*(μ,σ) for U(0,90°) and σ = (a) 5°, (b) 15°, and (c) 45°.

15°. As σ increases, however, this effect diminished and cell density converges to approximately the same value regardless of the value of μ. This result is reasonable: the corresponding ρ_β at different μ converges to the uniform distribution with an increasing σ (Fig. 5c). Also, when μ increases, it is more desirable to have a larger σ, because it means a higher proportion of nucleating sites have the desired smaller β. In summary, nucleating agents with conical crevices of small semiconical angles lead to higher cell density. Using eq. (2), Figure 7 indicates that the optimal size of β, for the particular materials system being studied, is 2.15°.

Effect of β distribution on cell size distributions

Plastic foams with narrower cell size distributions tend to have better mechanical properties. From Figure 8, it is apparent that the skewness of ρ_β does not

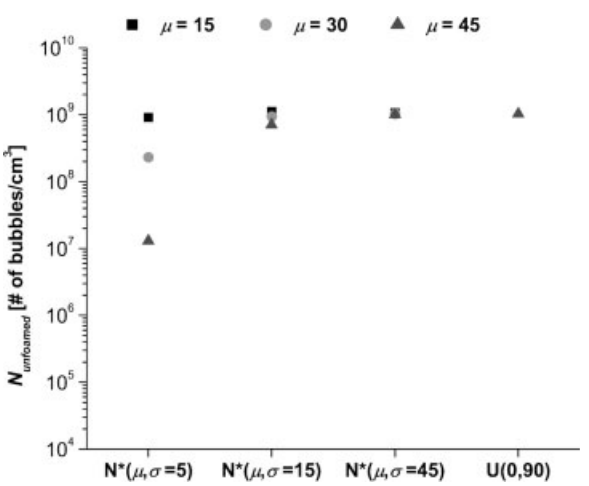

Figure 6 Effect of surface geometries on cell density.

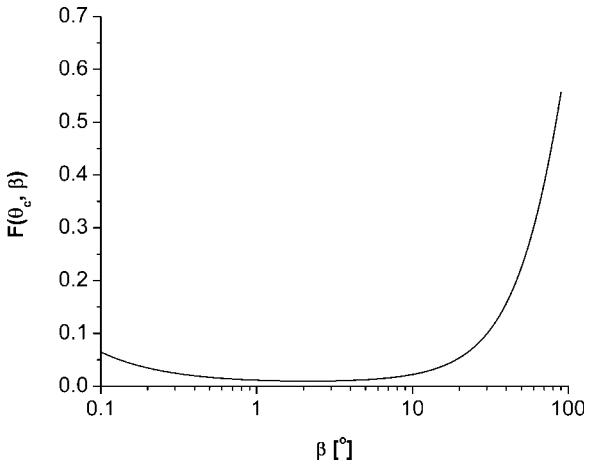

Figure 7 Effect of β on $F(\theta_c, \beta)$ [$\theta_c = 85.7^\circ$].

have a noticeable effect on cell size distribution except at a low dispersion of β (i.e., $\sigma = 5^\circ$). When $\sigma = 5^\circ$, narrow cell size distribution and a smaller cell size is observed when ρ_β is skewed toward a smaller β angle. On the other hand, for a larger σ (i.e., $\sigma = 15^\circ$), cell size distribution becomes invariant to further increase of σ, regardless of the value of μ.

Relationship between cell size distribution and cell density

Figure 9 demonstrates the relationship between the cell size distribution and the cell density, namely that cell size distribution decreases with increasing the cell density. Therefore, nucleating agents with conical crevices of small semiconical angles not only lead to a higher cell density, but also to narrower cell distribution and a smaller cell size, which are both desirable qualities for plastic foams.

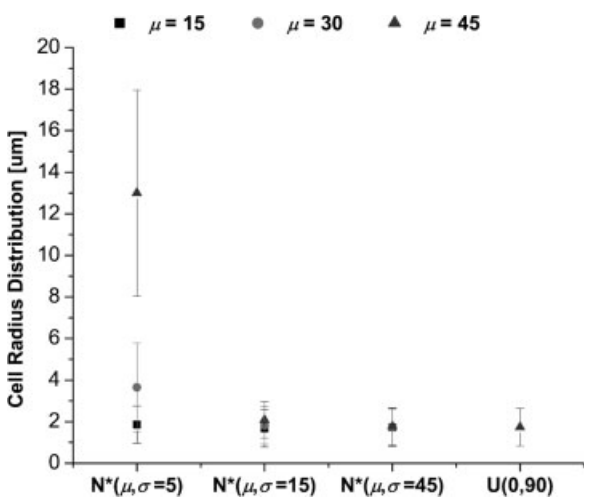

Figure 8 Effect of surface geometries on cell size distribution.

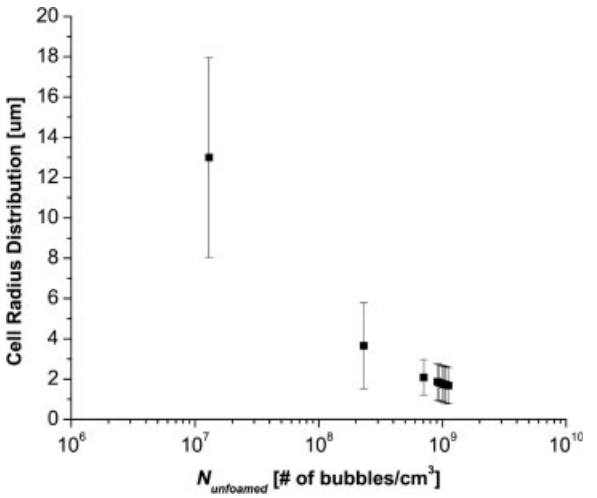

Figure 9 Cell size distribution versus cell density.

CONCLUSIONS

The effects of the surface geometry of nucleating agents on the quality of plastic foams were studied using computer simulations of a PS/CO_2 foaming system. Nucleating sites were approximated as conical crevices with various distributions of semiconical angles. It was shown that nucleating agents with many crevices of small semiconical angles lead to higher quality polymer foams, with a high cell density, a smaller cell size and narrower cell size distribution.

The authors are grateful to the Consortium of Cellular and Micro-Cellular Plastics (CCMCP), AUTO21, and the Natural Sciences and Engineering Research Council of Canada (NSERC) for their financial support of this project.

NOMENCLATURE

A_{het}	Surface area of nucleating agents per unit volume of polymer melt, m^2/m^3
C	Dissolved gas concentration in the polymer-gas solution, mol/m^3
C_{avg}	Average gas concentration in the polymer-gas solution, mol/m^3
F	Ratio of the volume of the nucleated bubble to the volume of a spherical bubble with the same radius, dimensionless
J_{het}	Heterogeneous nucleation rate (per unit area of nucleating agent), $\#/m^2$ s
J_{hom}	Homogeneous nucleation rate (per unit volume of polymer), $\#/m^3$ s
k_B	Boltzmann constant, m^2kg/s^2 K
M	Molecular mass of gas molecules, kg
N_A	Avogadro's number, #/mol
$N_{b,unfoam}$	Cell density with respect to unfoamed volume, $\#/m^3$ s

P_{bub}	Bubble pressure, Pa
$P_{bub,cr}$	Bubble pressure of a critical bubble, Pa
P_{sys}	System pressure, Pa
Q	Ratio of the surface area of the nucleated bubble to the surface area of a spherical bubble with the same radius, dimensionless
R_{bub}	Bubble radius, m
R_g	Universal gas constant, J/K mol
t	Current time, s
t'	Time at which a bubble is nucleated, s
T_{sys}	System temperature, K
β	Semi-conical angle of a heterogeneously nucleating site, degrees
γ_{lg}	Surface tension at the liquid-gas interface, N/m
θ_c	Contact angle, degrees
ρ_β	Probability density function of β, dimensionless

References

1. Seeler, K. A.; Kumar, V. J Reinforced Plast Comp 1993, 12, 359.
2. Collias, D. I.; Baird, D. G.; Borggreve, R. J. M. Polymer 1994, 25, 3978.
3. Collias D. I.; Baird, D. G. Polym Eng Sci 1995, 35, 1167.
4. Collias D. I.; Baird, D. G. Polym Eng Sci 1995, 35, 1178.
5. Doroudiani, S.; Park, C. B.; Kortschot, M. T. Polym Eng Sci 1998, 38, 1205.
6. Matuana, L. M.; Park, C. B.; Balatinecz, J. J Polym Eng Sci 1998, 38, 1862.
7. Suh, K. W.; Park, C. P.; Maurer, M. J.; Tusim, M. H.; Genova, R. D.; Broos, R.; Sophiea, D. P. Adv Mater 2000, 12, 1779.
8. Kabumoto, A.; Yoshida, N.; Itoh, M.; Okada, M. U.S. Pat. 5,844,731 (1998).
9. Hansen, R. H.; Martin, W. M. Ind Eng Chem Prod Res Dev 1964, 3, 137.
10. Hansen, R. H.; Martin, W. M. J Polym Sci Part B: Polym Lett 1965, 3, 325.
11. Yang, H. H.; Han, C. D. J Appl Polym Sci 1984, 29, 4465.
12. Wilkenlog, F. N.; Wilson, P. A.; Fox, S. A. U.S. Pat. 4,107,354 (1978).
13. Han, C.D.; Kim, Y. W.; Malhotra, K. D. J Appl Polym Sci 1976, 20, 1583.
14. Needham, D. G. U.S. Pat. 5,366,675 (1994).
15. Ehrenfruend, H. A. U.S. Pat. 1,102, 69 (1978).
16. Alteepping, J.; Nebe, J. P. U.S. Pat. 4,940,736 (1990).
17. Park, J. J.; Katz, L.; Gaylord, N. G. U.S. Pat. 5,116,881 (1990).
18. Ma, C. Y.; Han, C. D. J Appl Polym Sci 1993, 28, 2983.
19. Johnson, D. E.; Krutchen, C. M.; Sharps, V. U.S. Pat. 4,424,287 (1984).
20. Ramesh, N. S.; Kweeder, J. A.; Rasmussen, D. H.; Campbell, G. A. SPE ANTEC Tech Papers 1992, 1078.
21. Ramesh, N. S.; Rasmussen, D. H.; Campbell, G. A. Polym Eng Sci 1994, 34, 1685.
22. Ramesh, N. S.; Rasmussen, D. H.; Campbell, G. A. Polym Eng Sci 1994, 34, 1698.
23. Colton, J. S. Materials & Mfg. Processes 1989, 4, 253.
24. Colton, J. S.; Suh, N. P. Polym Eng Sci 1987, 27, 493.
25. Allen, R. B; Avakian, R. W. U.S. Pat. 4,544,677 (1985).
26. Lee, S. T. Polym Eng Sci 1993, 33, 418.
27. Park, C. B.; Cheung, L. K.; Song, S. W. Cellular Polym 1998, 17, 221.
28. Naguib, H. E.; Park, C. B.; Lee, P. C. J Cellular Plast 2003, 39, 2231.
29. Zeng, C.; Han, X.; Lee, L. J.; Koelling, K. W.; Tomasko, D. L. Adv Mater 2003, 15, 1743.
30. Stauss, W.; D'souza, N. A. J Cellular Plast 2004, 40, 229.
31. Nam, P. H.; Maiti, P.; Okamoto, M.; Kotaka, T.; Nakayama, T.; Takada, M. Polym Eng Sci 1907, 2002, 42.
32. Mitsunaga, M.; Ito, Y.; Ray, S. S.; Okamoto, M.; Hironako, K.; Macromol Mater Eng 2003, 288, 543.
33. Shen, J.; Zeng, C.; Lee, J. Polymer 2005, 46, 5218.
34. McClurg, R. B. Chem Eng Sci 2004, 59, 5779.
35. Leung, S. N.; Park, C. B.; Li, H.; Plast Rubber Compos: Macromol Eng 2006, 35, 93.
36. Leung, S. N.; Park, C. B.; Li, H. J Appl Polym Sci 2007, 104, 902.
37. Wilt, P. M. J Colloid Interface Sci 1986, 112, 530.
38. Blander, M.; Katz, J. L. AIChE J 1975, 21, 833.
39. Leung, S. N.; Park, C. B.; Xu, D.; Li, H.; Fenton, R. G. Ind Eng Chem Res 2006, 45, 7823.
40. Sanchez, I. C.; Lacombe, R. H. Macromolecules 1978, 11, 1145.
41. Leung, S. N.; Wong, A.; Park, C. B. SPE ANTEC Tech Papers 2007, 302659.